Volume 13
Number 47
21 December 2022
Pages 6417-6566

Polymer Chemistry

rsc.li/polymers

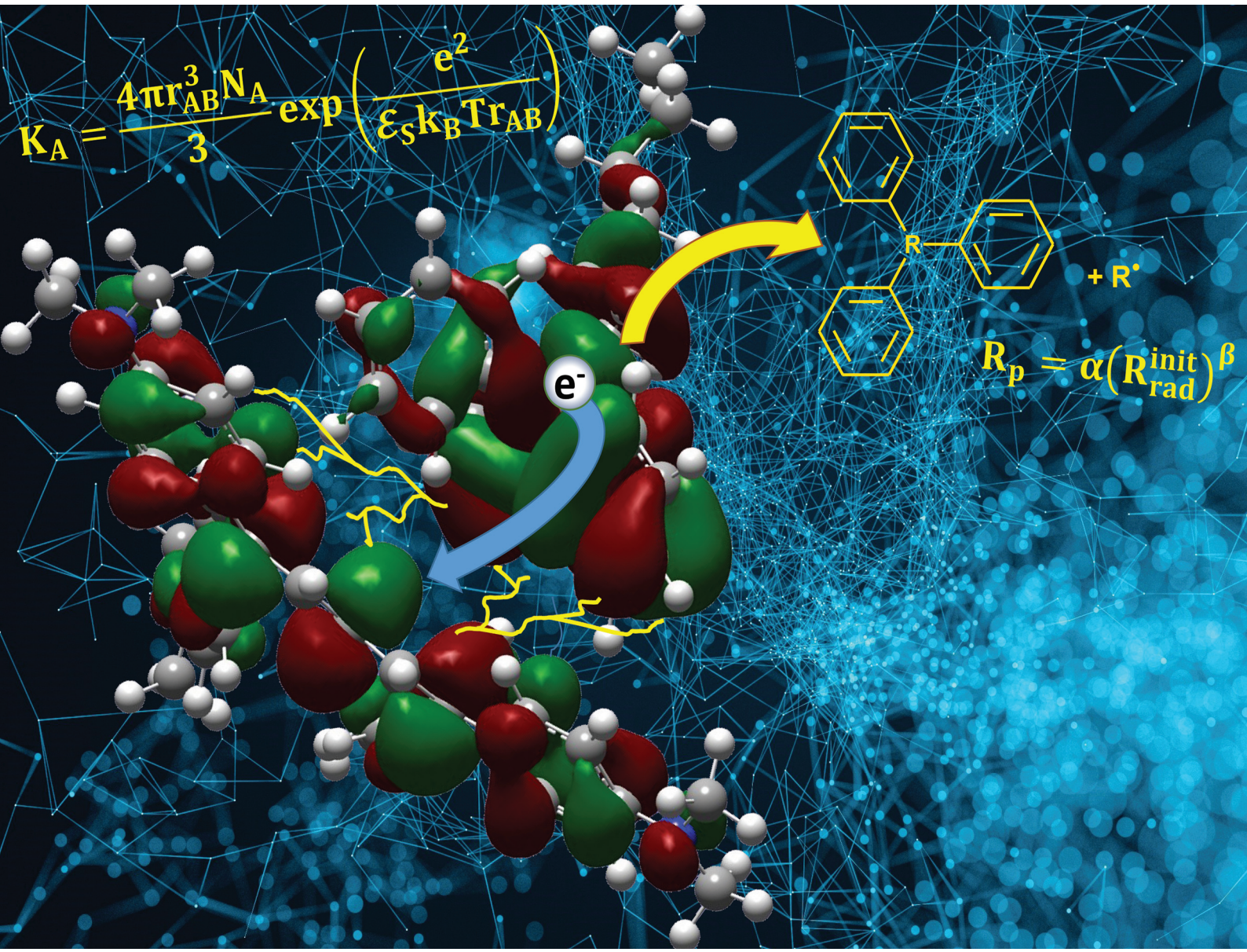

ISSN 1759-9962

ROYAL SOCIETY OF CHEMISTRY

PAPER

Xavier Allonas *et al.*

A highly sensitive photoinitiating system based on pre-associated ion-pairs for NIR radical photopolymerization of optically clear materials

Polymer Chemistry

ROYAL SOCIETY OF CHEMISTRY

PAPER

View Article Online
View Journal | View Issue

Cite this: *Polym. Chem.*, 2022, **13**, 6475

A highly sensitive photoinitiating system based on pre-associated ion-pairs for NIR radical photopolymerization of optically clear materials†

Junyi Zhou, [a] Lena Pitzer,[b] Christian Ley, [a] Thomas Rölle[b] and Xavier Allonas *[a]

A new highly reactive photoinitiating system based on a penta-methine cyanine dye and a triarylalkylborate salt for radical photopolymerization reactions using near infra-red (NIR) light was investigated. The remarkably high reactivity is partly ascribed not only to the photochemical properties of the dye such as its very high absorption coefficients but also to the combination of the dye with the borate salt. Interestingly, the correlation between the borate salt concentration and the rate of polymerization can be displayed in a saturation graph. This effect is presumably caused by the formation of an ion-pair complex consisting of the cationic dye and anionic borate molecule in a medium of moderate polarity. It is shown that the association constant of such ion-pairs is quite high and, due to the short lifetime of the excited state of the dye, it is the only possible route for the generation of initiating radicals after excitation. Finally, it is found that the rate of polymerization correlates with the calculated rate of initiation, giving confidence to the proposed initiation mechanism. Advantageously, the high sensitivity of the new photoinitiating system allows for the use of a low LED light power of 40 mW cm^{-2} and thus supports a truly photonic mechanism of initiation instead of a thermal one.

Received 28th March 2022,
Accepted 26th August 2022

DOI: 10.1039/d2py00384h

rsc.li/polymers

1. Introduction

Currently, the initiation of a polymerization reaction *via* light is indispensable in a plethora of applications. During the last decade, NIR light sensitized photopolymerization especially has attracted increasing attention.[1–3] This is mainly due to the fact that NIR radiation is less harmful in comparison to UV- and visible light and is not commonly absorbed by organic molecules, leading to less interference during irradiation and, ideally, the respective photopolymers do not require a dark environment during operation.[4–14] Only special NIR dyes are prone to convert NIR rays into polymerization initiators with suitable coinitiators. Amongst these, particularly penta- and hepta-methine cyanine dyes were recently utilized for photopolymerizations due to their high molar absorptivity and rather benign synthetic availability. Another remarkable property of NIR dyes is their much lower fluorescence quantum yields in comparison to dyes used for UV- or visible light photopolymerizations. A low fluorescence quantum yield signifies that a major proportion of the absorbed light is emitted as heat. This fact has been applied advantageously in many recent polymerization studies where the NIR dye caused the occurrence of a thermal polymerization reaction after irradiation. For example, it was demonstrated that NIR dyes in combination with iodonium salts and thermal initiators form an initiating system reaching polymerization conversions of greater than 80%, even for methacrylic resins.[12] However, a rather high light intensity of 400 mJ cm^{-2} is required and, moreover, the temperature increases during polymerization up to 120 °C or higher. Also, a recent paper reported a similar NIR light-sensitized thermal polymerization protocol. In another recent study, a much lower light intensity of 100 mW cm^{-2} could be used to enable a photoinduced ATRP process in the NIR region (790 nm), leading to good control of the molecular weight and a low dispersity.[7] These initiating systems are clearly beneficial in terms of replacing oven processes or for thermally stable applications; however, they are not useful for heat sensitive applications. Until now, there is no report about a truly photonic NIR light-initiated photopolymerization protocol that operates with only low light intensities. In this study, we present such a highly reactive NIR light sensitive photoinitiating system based on a combination of a cationic penta-methine cyanine dye and triarylalkylborate salts.

Even though triphenylalkylborate salts of cyanines have already been found to be excellent photoinitiators a long time

[a]*Laboratoire de Photochimie et d'Ingénierie Macromoléculaires, Institut Jean Baptiste Donnet, 3b rue Alfred Werner, 68093 Mulhouse Cedex, France.*
E-mail: xavier.allonas@uha.fr
[b]*Covestro Deutschland AG, Specialty Films – Research and Development, 51365 Leverkusen, Germany*

† Electronic supplementary information (ESI) available. See DOI: https://doi.org/10.1039/d2py00384h

ago, the use of this dye/coinitiator combination has only been applied to visible light photopolymerizations[15–18] and limited efforts have been devoted to the use of borates as coinitiators in the NIR region.

In this study, photopolymerization experiments were performed using a polymethine cyanine dye – in the following sections called IRT – absorbing in the NIR range of the electromagnetic spectrum, and triarylalkylborate salts as coinitiators (Scheme 1). An unexpected dependency of the maximum rate of polymerization on the coinitiator concentration was found. Photochemical insights are given that account for the high reactivity of this photoinitiating system. A model based on the preassociation of the positively charged dye with the negatively charged borate is proposed. Calculated association constants were used to determine the rates of initiation that perfectly correlate with the rates of polymerization. Additionally, exceptional photobleaching occurs during irradiation, finally leading to optically transparent materials, thus enlarging the application opportunities for this NIR-sensitive photoinitiating system.

2. Experimental

2.1. Materials

Karenz IRT, Karenz P3B (B5) and Karenz N3B (B3) were purchased from Showa Denko Europe GmbH. Acetonitrile and dimethylsulfoxide (DMSO) were purchased from Merck Sigma-Aldrich. Ethoxylated (3) bisphenol-A dimethacrylate was a gift from Sartomer (SR 349). The polyol (Acclaim Polyol 6300) was provided by Covestro.

2.1.1. General procedure for the synthesis of triarylalkylborates.[19–21] A four-neck flask equipped with a reflux condenser, a thermometer, a dripping funnel and a stirring bar was charged under an inert atmosphere with diisopropylhexylborate (1.0 eq.) and magnesium turnings (3.0 eq.). A solvent mixture consisting of anhydrous toluene and anhydrous THF (5.8 : 1, 1.9 M) was added to the flask and the mixture was stirred for 30 min at ambient temperature. The corresponding bromoarene was added dropwise to this suspension until the exothermicity was increased, indicating the start of the reaction; however, for this step a maximum quantity of 10% of bromoarene was used. The residual bromoarene was diluted in a solvent mixture consisting of dry toluene and dry THF (1 : 1, the end molarity of the reaction was 0.4 M) and it was then continually added dropwise to the reaction mixture without allowing the temperature to rise above 45 °C. After complete addition, the reaction mixture was heated under reflux for 1 h or until all magnesium turnings were dissolved. The reaction mixture was allowed to cool to room temperature before being poured onto a mixture of ice and tetrabutylammonium bromide (1 eq.). This mixture was stirred for 1 h. After phase separation, the organic phase was washed many times with water until a bromide test (HNO_3 (aq., 10%) + $AgNO_3$) indicated the absence of any bromide. The organic phase was concentrated under a vacuum and the raw product recrystallized from methanol to yield the pure product (for details, see the ESI†).

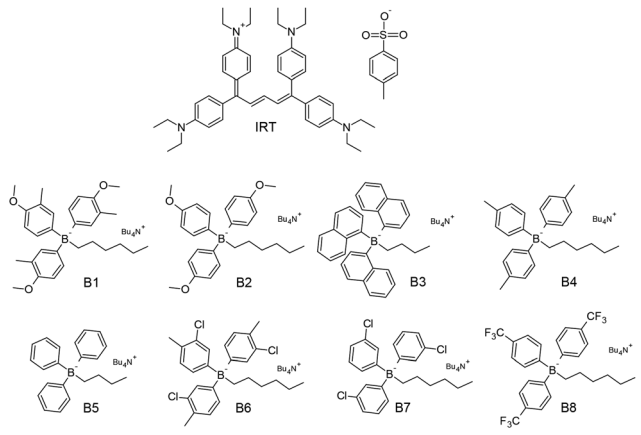

Scheme 1 Penta-methine cyanine dye IRT and borate coinitiators used in this study (Bu_4N^+ stands for the tetrabutylammonium cation).

2.2. Computation

A computational study was performed at the density functional theory level (DFT) using the Gaussian 16 set of programs at the Mésocentre of Strasbourg. The energies were computed at the M062X/6-311++G**//M062X/6-31G* level of theory. The same level was used for time-dependent calculations. Frequencies were computed at the M062X/6-31G* level.

2.3. Experimental methods

Photopolymerization reactions were performed using ethoxylated (3) bisphenol-A dimethacrylate. 10 wt% of DMSO was added to improve the solubility of IRT, thereby reducing the viscosity of the medium to 200 mPa s. The concentration of initial double bonds in the formulation was 4.52 M. The NIR irradiation was performed using a LED (Thorlabs, M850C3) emitting at 850 nm with an irradiance reduced to 40 mW cm^{-2}.

The change in double bond conversion of the acrylate was monitored by real-time FTIR using a Vertex 70 from Bruker Optics.[22] The acrylate formulation was sandwiched between two BaF_2 pellets using a spacer of 25 μm. The area of the double-bond vibration band was measured at 1640 cm^{-1} and the carbonyl band at 1730 cm^{-1} was used as a reference. The double-bond conversion (DBC) was then calculated according to the below equation:

$$\mathrm{DBC}\,(\%) = \left(1 - \frac{A_t^{1640}/A_t^{1730}}{A_0^{1640}/A_0^{1730}}\right) \times 100 \qquad (1)$$

The maximum rate of polymerization was calculated from the slope of the time plot at the inflexion point according to the below equation:

$$R_p = \frac{\mathrm{dDBC}}{\mathrm{dt}}\frac{[\mathrm{M}]_0}{100} \qquad (2)$$

A FluoroMax-4 (Horiba, Jobin–Yvon) spectrofluorimeter equipped with a near IR PMT coupled with a time correlated

single photon counting (TCSPC) accessory was used to measure steady-state fluorescence spectra and fluorescence decays. Steady-state spectra were obtained in acetonitrile using an internal xenon lamp as an excitation source. For fluorescence decays, an 823 nm nano LED with a pulse duration of 200 ps was used as a pulsed excitation source leading to a time resolution of around 100 ps after deconvolution.

Absorption spectra were recorded on a Specord 210 from Analytik Jena.

Oxidation and reduction potentials were measured as described in the literature using a 1.0 mm diameter platinum electrode as a working electrode and a AgCl/LiCl reference electrode in acetonitrile using tetrabutylammonium hexafluorophosphate as a supporting electrolyte.[23] The reduction potential of IRT was $E_{red} = -0.56$ V/SCE.

3. Results and discussion

3.1. Photopolymerization experiments

Photopolymerization experiments were performed using a two component photoinitiating system comprising the pentamethine cyanine dye IRT as the absorbing species and various triarylalkylborate salts as coinitiators in an acrylate formulation having a viscosity of 200 mPa s. Fig. 1 shows the time–conversion curves for the photopolymerization reactions utilizing different triarylalkylborate salts. This study gives clear evidence for a strong influence of the borate structure on the final conversion. Table 1 shows the maximum rate of polymerization as well as the maximum conversion obtained after 10 s of irradiation at 850 nm. It is worth noting that a relatively low intensity of light (40 mW cm^{-2}) was used for these experiments, in contrast to many studies in the field of NIR photopolymerization. For example, the system IRT/borate can be compared advantageously to a typical system using iodonium salt as a coinitiator and requiring 200–350 mW cm^{-2} to achieve an efficient photopolymerization.[10]

Formulations containing only the dye or the coinitiators did not exhibit any conversion after 30s of irradiation. As mentioned before, different reactivity behaviors can be observed for the different formulations containing both IRT and borate salts. First of all, the three borates B6, B7 and B8, having the highest oxidation potential, do not lead to any polymerization. In contrast to these, borate B1 with the lowest oxidation potential is very reactive leading to a maximum polymerization rate of $R_p^{max} = 1.68$ M s^{-1} with a maximum final conversion of $DBC_{max} = 41\%$. All other borates having an oxidation potential in between show good to moderate reactivity with maximum rates of conversion ranging from 1.31 M s^{-1} to 0.51 M s^{-1} and a maximum conversion of around 30%.

The dependency of the reactivity on the oxidation potential of the borate salt is shown in Fig. 2. This graph shows clearly a negative linear correlation up to the highest oxidation potential limit – here around 1.0 V *vs.* SCE. Any borate having a higher oxidation potential than this limit is not suitable for a photoinitiating system in combination with the NIR dye IRT.

This correlation gives clear evidence for an electron transfer reaction between the borate salt and the excited IRT dye and is consistent with the known reactivity of alkyl-substituted borate salts, which release alkyl radicals after electron transfer to the excited dye.[15,16]

Moreover, the delayed start of the polymerization in the case of the B4 and B5 borates is in line with the postulated generation of initiating radicals, since a successful overcoming

Table 1 Maximum rate of polymerization R_p^{max}, maximum conversion DBC^{max} and oxidation potential E_{ox} of borates used, obtained after 130 s of irradiation at 850 nm and 40 mJ cm^{-2}

Borate	R_p^{max} (M s^{-1})	DBC^{max} (%)	E_{ox} (V/SCE)
B1	1.68	41	0.47
B2	1.31	33	0.55
B3	0.98	28	0.72[a]
B4	0.68	33	0.72
B5	0.51	57	0.81[a]
B6	2×10^{-3}	3	1.08
B7	0	0	1.16
B8	0	0	1.42

[a] From ref. 18.

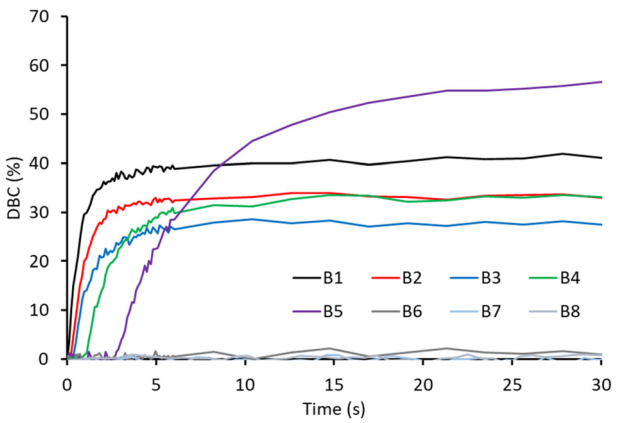

Fig. 1 Conversion–time curves of different borates at a concentration of 0.3 mol%.

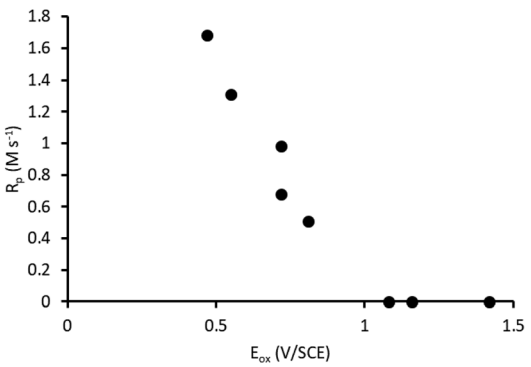

Fig. 2 Dependence of the rate of polymerization R_p on the oxidation potential E_{ox} of the borate salt.

of oxygen inhibition is only possible after the formation of a certain threshold concentration of initiating radicals.

To obtain a deeper understanding of the postulated initiating mechanism, further experiments were performed using the fastest reacting borate B1. Fig. 3a shows the time–conversion curves measured using different concentrations of borate B1. Interestingly, an unexpected change in the conversion curves can be observed. As can be seen, at first both the rate of polymerization and the final conversion increase with an increasing borate concentration. A slight decrease in the final conversion is observed for the highest borate concentration, probably because of the high concentration of hexyl radicals, which not only initiated the polymerization but could also decompose the dye (*vide infra*). However, it becomes obvious that a plateau value for the rate of polymerization R_p is obtained for a borate concentration higher than 2×10^{-2} M (Fig. 2b). This behavior cannot be explained in terms of conventional quenching of the excited state of the dye by the coinitiator since for a conventional dynamic quenching process, a quasi-linear correlation between the borate concentration and the rate of polymerization would be expected (see the ESI†).

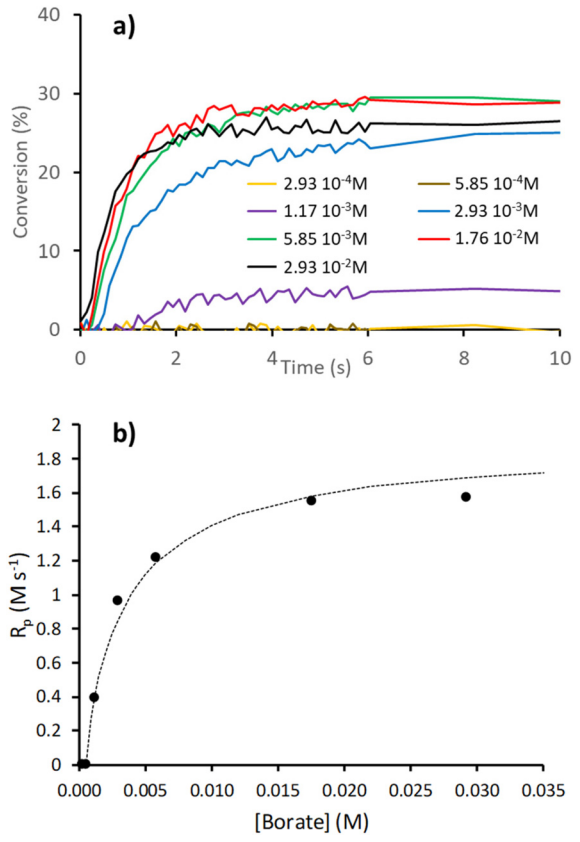

Fig. 3 (a) Conversion *vs.* time curves of formulations comprising SR 349 + 10% DMSO and different concentrations of borate B1 ([IRT] = 1.40×10^{-3} M) and (b) experimental changes in the rate of polymerization with the borate concentration and the corresponding best fit (see the text).

Cationic cyanine dyes are known to initiate photopolymerization reactions without the addition of a coinitiator if the counter-ion of cyanine is a borate anion.[15,16] In the present case, a borate salt is added as a coinitiator and the tosylate anion of the IRT dye acts as a weakly coordinating counter-ion. This would suggest that a diffusion process must take place after excitation to create radicals through the bimolecular electron transfer process between the dye cation and the borate anion. Since this diffusion based dynamic quenching mechanism cannot be valid in the present case as deduced before, the system needs to be studied in more depth. Therefore, it is necessary to collect some data about the reactive excited state of the used NIR dye IRT.

3.2. Photochemical insights

To the best of our knowledge, the photochemistry of IRT has not been reported and the behavior of this dye has scarcely been studied as a photoinitiator.[24,25] Therefore, gathering some information about the properties of this dye is a prerequisite, particularly concerning its singlet excited state. The absorption spectrum of IRT in acetonitrile is shown in Fig. 4. Interestingly, two important absorption bands appear in the IR and NIR regions with extremely high absorption coefficients. In acetonitrile, the maxima of absorption are located at 815 nm and 643 nm with absorption coefficients ε of 1.35×10^5 M^{-1} cm^{-1} and 4.8×10^4 M^{-1} cm^{-1}, respectively. Since this absorption spectrum extends from 550 nm to 900 nm, sensitization in the visible region could be possible.

Although the band centered at 815 nm corresponds clearly to the S_0–S_1 electronic transition, the question arises about the nature of the band centered at 643 nm. The computation at the M062X/6-311++G**//M062X/6-31G* level of the S_0–S_1 electronic transition predicts an intense transition (oscillator strength f = 1.13) with an overestimated vertical transition at 2.09 eV (exp.: 1.52 eV). It is known that DFT methods overestimate the vertical transition of highly delocalized π chromophores. Therefore, the vibrationally resolved electronic spectrum of the S_0–S_1 absorption band was computed and reported using the experimental vertical energy of the transition (Fig. 4 (a)). As can be seen, the more red-shifted band at 815 nm was predicted with excellent accuracy. Both the absorption coefficient and the full width at half maximum are similar to the measured ones (numbers of coefficients and FWHM). More interestingly, the absorption band at 643 nm is also predicted to belong to the same S_0–S_1 band. Also here, the prediction is in good agreement with the experimental data in terms of absorption coefficients (1.34×10^4 M^{-1} cm^{-1} and 4.8×10^4 M^{-1} cm^{-1}, respectively) and maximum wavelengths of absorption (644 nm and 643 nm, respectively). A larger deviation in the absorption coefficient of the band at 643 nm could arise from an anharmonicity of the vibrations, which was not taken into account in the calculation. Fig. 4c shows that this band is mainly a HOMO–LUMO transition between strongly delocalized π and π* orbitals.

Moreover, the fluorescence spectra obtained by exciting the IRT dye at 636 nm and 751 nm overlap perfectly showing only

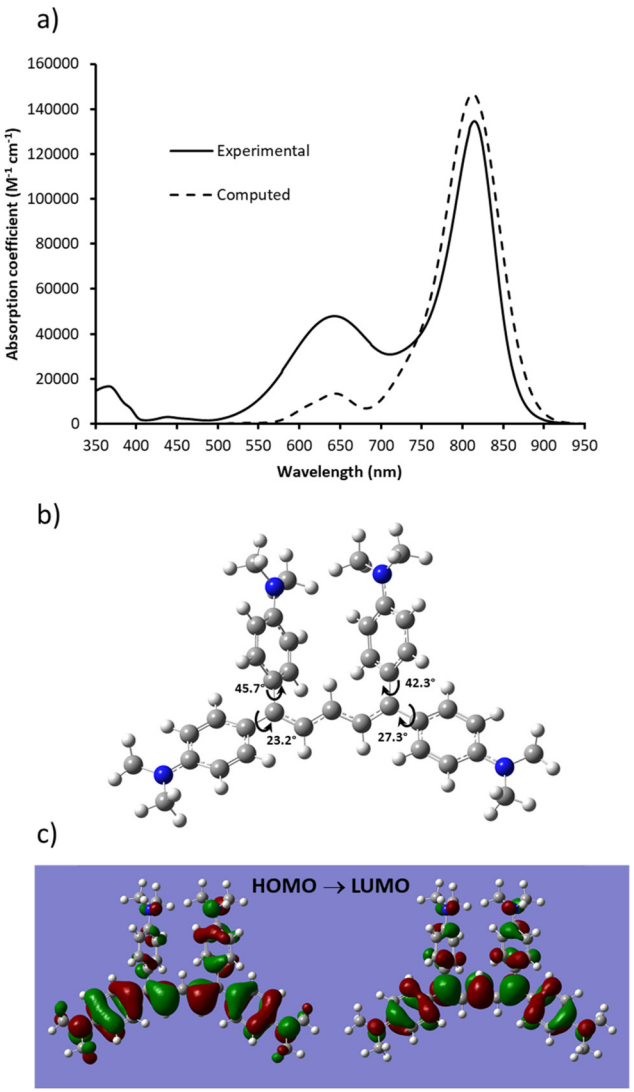

Fig. 4 (a) Experimental and computed absorption spectra of IRT in acetonitrile, (b) structure of IRT in the gas phase and (c) a computed HOMO–LUMO electronic transition.

one emissive state in the dye. Furthermore, the measured quantum yields of fluorescence by exciting the sample at the two aforementioned wavelengths give the same values of quantum yields (Φ_f = 0.077 and 0.075, in a polyol solution, respectively).

Having clarified the nature of the 500–900 nm absorption of IRT, it is now possible to determine important photophysical and photochemical data. First of all, integration of the absorption band allows for the determination the oscillator strength f:[26–28]

$$f = 4.32 \times 10^{-9}\, n^2 \int \varepsilon(\bar{\nu})\, d\bar{\nu} = 1.19 \quad (3)$$

with n being the refractive index of acetonitrile (n = 1.337) and $\bar{\nu}$ the frequency. The oscillator strength is found to be very high with a value reaching unity. The agreement with the previously computed value is excellent. From this value, the transition dipole moment μ is calculated as:

$$\mu = \sqrt{\frac{3he^2 f}{8\pi^2 m_e c\bar{\nu}}} = 14.4\ \text{Debye} \quad (4)$$

with e being the charge of the electron and m_e its mass. The value of the dipole moment μ gives an indication about a potential charge transfer during light absorption. Very interestingly, this allows the evaluation of the natural lifetime, *i.e.* the lifetime that the singlet state should have considering only fluorescence as a decay pathway:

$$\tau_r{}^0 = 3.417 \times 10^8 / \bar{\nu}_{max}{}^2 n^2 \int \varepsilon(\bar{\nu})\, d\bar{\nu} \quad (5)$$

The natural lifetime of 8.24 ns permits the calculation of the fluorescence rate constant:

$$k_f = \frac{1}{\tau_r{}^0} = 1.21 \times 10^8\ s^{-1} \quad (6)$$

The actual fluorescence lifetime (τ_F) was measured in different solvents and the results are presented in Table 2. In low viscous solvents, the fluorescence decay is similar to the response of the setup, which prevents any measurement of τ_F < 0.2 ns. In viscous media, the signal is very close to a single exponential decay and was fitted accordingly. As can be seen, the singlet excited state decays in less than 1 ns even in a viscous solvent as a result of the free rotation of C–C bonds in the singlet excited state of the cyanine dye.[29] Fluorescence quantum yields (ϕ_F) were also measured in the same solvents (Table 2). It can be seen that the values obtained are very low with the value in the polyol of *ca.* 9% being the highest one. This is in agreement with the estimation, which could be made from the calculation of the photophysical properties and the measured fluorescence lifetime. Indeed, assuming a gross value of 0.8 ns in a viscous solvent, the fluorescence quantum yield can be evaluated from:

$$\phi_f = k_f \tau_f \quad (7)$$

Using the lifetime and quantum yield measured in the polyol, this calculation yielded a value for the fluorescence rate constant $k_f = 1.0 \times 10^8\ s^{-1}$, which is in perfect agreement with the previously calculated value.

No triplet state was detected using laser flash photolysis, as can be expected from such a highly conjugated molecule with many possible internal rotational decay pathways from the excited state.

Taking into account that the singlet excited state lifetime is very short and that the viscosity η of the medium is high, the

Table 2 Experimental fluorescence lifetime and quantum yields obtained in different solvents

	Acetonitrile	Polyol	SR 349	SR 349 + DMSO
τ_F (ns)	<0.2	0.87	0.96	0.63
ϕ_F	0	0.089	0.077	0.025

photosensitivity of the dye/borate mixture as a photoinitiating system is very good. From the singlet state lifetime in the resin (τ_f = 0.63 ns), the degree of quenching DE by the borate can be calculated, which is actually the quantum yield of radicals created through dynamic quenching:

$$DE = 1 - \frac{1}{1 + k_q \tau_0 [\text{Borate}]} \quad (8)$$

Using a borate concentration of 1.76×10^{-2} M and assuming that the quenching is diffusion controlled, the use of the above-mentioned Stokes–Einstein equation for the calculation of the diffusion rate constant leads to a degree of quenching DE = 0.04%. Therefore, the predominant non-radiative deactivation pathway reduces the excited state lifetime to about 0.63 ns, a value that is too low to allow efficient dynamic quenching.

This result supports the previously mentioned hypothesis that dynamic quenching hardly takes place and cannot account for the high efficiency of IRT/borate systems. Although some cyanine/borate pairs were already reported to have good reactivity in the visible region, it is surprising that a simple mixture as in this study could reach the same efficiency. It is therefore interesting to evaluate the possibility of a pre-association of the dye and the borate in the viscous medium.

3.3. Pre-association effect

Due to the high viscosity and moderate polarity of the used acrylate photopolymerizable resin, the presence of either geminate ion pairs and/or free ions is possible. In relation to this study, this means that the IRT-tosylate and ammonium-borate pairs can also be dissociated, leading to a possible association of an IRT-borate pair. Following this, the photopolymerization can either be initiated by the IRT-tosylate (IRT···T) pair (route 1 in Scheme 2), the free IRT cation (route 2 in Scheme 2), or the IRT-borate (IRT···B) pair (route 3 in Scheme 2). In the case of the free IRT and the IRT-tosylate pair, a diffusion process must take place after excitation in order to favor the dynamic quenching by the borate. It was seen above that this process is not efficient due to the low degree of quenching. In the case of the IRT-borate pair, light absorption instantaneously leads to static quenching. Thus, three reaction pathways can be competitive, depending on the viscosity of the resin and the association constants of the ion-pairs (Scheme 2).

This process is governed by the association constants of IRT-borate ion-pair formation $K_{(IRT\cdots B)}$ and IRT-tosylate ion-pair formation $K_{(IRT\cdots T)}$. From a general point of view, the association constant K_A of ion pairs can be evaluated from the work of Fuoss and Eigen.[30–32] In this approach, only the coulombic interaction is taken into account and the solvent is assumed to be a dielectric continuum:

$$K_A = \frac{4\pi r_{AB}{}^3 N_A}{3} \exp\left(\frac{e^2}{\varepsilon_S k_B T r_{AB}}\right) \quad (9)$$

with r_{AB} being the sum of the radii r_A and r_B of the ions A and B, respectively, T the temperature, e the electron charge and ε_S the dielectric constant of the medium. The radii of the ions r_A and r_B were calculated from the volume of the molecule as evaluated from the surface accessible to a solvent molecule radius of 1.4 Å. The calculation was made using B5 as a reference. The association constants for the dye-borate ($K_{(IRT\cdots B)}$) and dye-tosylate ($K_{(IRT\cdots T)}$) pairs are shown in Table 3, assuming a dielectric constant of ε_S = 11.0 for the SR349/DMSO mixture (see the ESI†).

It can be seen that a pre-association between the cationic IRT and the borate anion could take place in an acrylate medium. Therefore, it can be expected that the dye-borate ion-

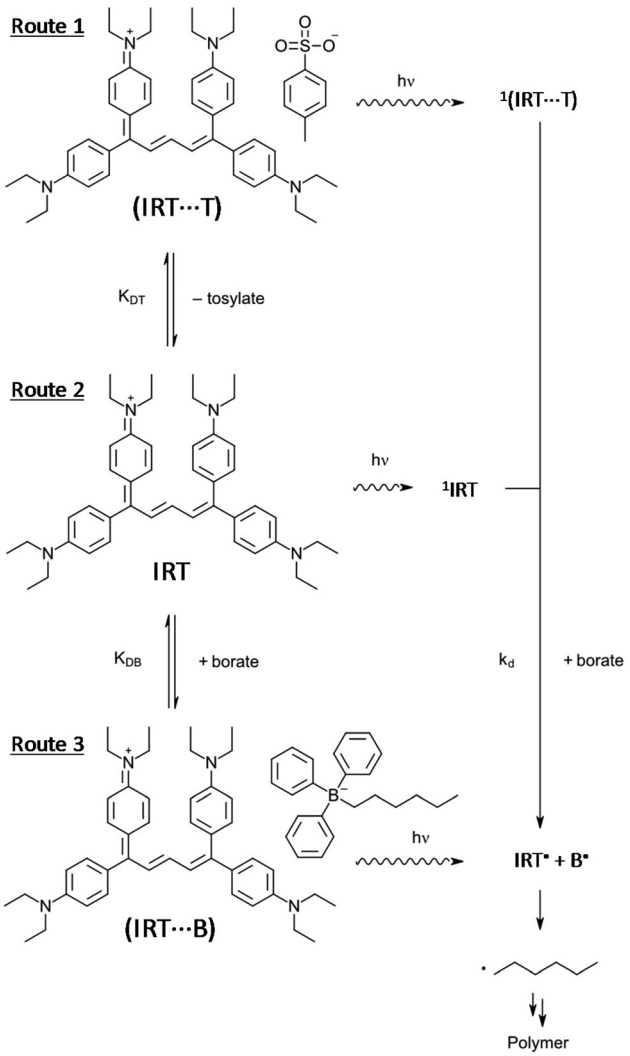

Scheme 2 Competitive radical formation mechanisms.

Table 3 Radii of the different ions involved in the reaction and the association constant K_A between the dye and the anions

Molecule	Radius (Å)	K_A (M^{-1})
IRT cation	7.28	
Triphenylbutylborate	6.36	270
Tosylate	4.87	300

pairs could lead to a static quenching under irradiation. Obviously, there is a competition between the association of the dye with tosylate and triphenylbutylborate, as shown in Scheme 2, leading to:

$$K_{(\mathrm{IRT}\cdots\mathrm{B})} = \frac{[(\mathrm{IRT}\cdots\mathrm{B})]}{[\mathrm{IRT}][\mathrm{B}]} \text{ and } K_{(\mathrm{IRT}\cdots\mathrm{T})} = \frac{[(\mathrm{IRT}\cdots\mathrm{T})]}{[\mathrm{IRT}][\mathrm{T}]} \quad (10)$$

where $[B] \sim [B]_0$ refers to the initial concentration of borate, which is higher than the concentration of dye, and $[IRT]_0 = [T]_0$ refers to the initial concentration of IRT and tosylate, respectively (1.4×10^{-3} M). Taking the initial 1 wt% as the initial concentration of borate (1.76×10^{-2} M), the final concentration of each species can be found by solving numerically the previous set of equations, leading to:

The concentration of free dye: $[IRT] = 2.4 \times 10^{-4}$ mol L^{-1}.

The concentration of free borate: $[B] = 1.65 \times 10^{-2}$ mol L^{-1}.

The concentration of dye-borate ion pair: $[(IRT\cdots B)] = 1.07 \times 10^{-3}$ mol L^{-1}.

Therefore, using the above-mentioned concentrations, a fraction $\Phi^{\text{ion-pair}} = 0.76$ of IRT is complexed with the borate at room temperature.

The absorption coefficient ε of IRT is 48 000 M^{-1} cm^{-1} at the light wavelength used of 850 nm. The dye-borate ion-pair should exhibit very close absorption properties as no change in the absorption spectrum is observed when the borate is added to a solution of the dye. The rate of formation of the excited state R_{exc} is:

$$R_{\text{exc}} = I_0(1 - 10^{-\varepsilon d[\mathrm{D}]})/d \quad (11)$$

with I_0 being the incident irradiance and d the photopolymer thickness of 20 μm. Assuming an irradiance of 40 mW cm^{-2} at 850 nm, this leads to a rate of $R_{\text{exc}} = 3.7 \times 10^{-2}$ mol dm^{-3} s^{-1}. It is expected that every excited dye-borate ion-pair leads to one butyl initiating radical. Therefore, one can assume that the rate of formation of radicals from the ion-pair $R_{\text{rad}}^{\text{ion-pair}}$ in such conditions is:

$$R_{\text{rad}}^{\text{ion-pair}} = I_0(1 - 10^{-\varepsilon d[\mathrm{DB}]})/d \quad (12)$$

The change in the rate of conversion with the borate concentration (Fig. 3) can be explained by an increase of the fraction of the dye-borate ion pair $\Phi^{\text{ion-pair}}$. Indeed, Fig. 5a shows that for $\Phi^{\text{ion-pair}} \leq 0.09$, the rate of conversion is zero. This could be attributed to the oxygen inhibition frame where most initiating radicals are scavenged by oxygen molecules instead of starting a polymerization reaction. As the IRT concentration is similar to that of dissolved oxygen (around 10^{-3} M), no polymerization is observed. In contrast for $\Phi^{\text{ion-pair}} \geq 0.1$, the rate of conversion increases until a plateau is observed for $\Phi^{\text{ion-pair}} \sim 0.8$. This corresponds to the maximum rate of conversion that could be reached at this dye concentration.

Table 4 shows the rates of conversion obtained from photopolymerization experiments performed using different concentrations of borate B1. Calculated dye-borate ion-pair concentrations [(IRT···B)] and the fraction of dye-borate ion-pair $\Phi^{\text{ion-pair}}$ values show that dye complexation increases with borate concentration, as expected. More interestingly, it could also be seen that the values for the rate of formation of initiating radicals $R_{\text{rad}}^{\text{ion-pair}}$ increase with $\Phi^{\text{ion-pair}}$.

Taking into account that below a borate concentration of $[B] = 5.8 \times 10^{-4}$ M, oxygen inhibition will not be overcome, the rate of initiation does not equal the rate of the formation of initiating radicals $R_{\text{rad}}^{\text{ion-pair}}$. In order to obtain a value for the rate of initiation, the rate of the formation of initiating radicals

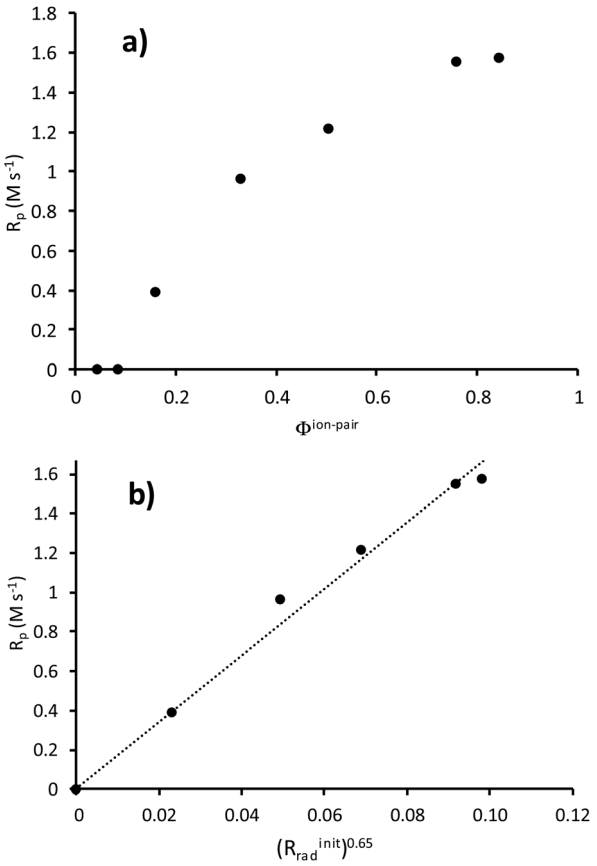

Fig. 5 (a) Saturation effect obtained for a high fraction of complexation between IRT and the borate and (b) the relationship between the rate of conversion and the calculated rate of initiation (see the text).

Table 4 Maximum rate of polymerization $R_p^{\max}$ obtained during the photopolymerization of SR349 + 10% DMSO with 1.4×10^{-3} M of dyes and different concentrations of B1 as borates. [(IRT···B)]: concentration of dye-borate ion pairs, $\Phi^{\text{ion-pair}}$: fraction of dye-borate ion pairs, $R_{\text{rad}}^{\text{ion-pair}}$: rates of the formation of radicals from the ion-pair, and $R_{\text{rad}}^{\text{init}}$: corrected rates of initiation

[Borate] (10^{-4} M)	$R_p^{\max}$ (M s^{-1})	[(IRT···B)] (10^{-4} M)	$\Phi^{\text{ion-pair}}$	$R_{\text{rad}}^{\text{ion-pair}}$ (10^{-2} M^{-1} s^{-1})	$R_{\text{rad}}^{\text{init}}$ (10^{-2} M^{-1} s^{-1})
2.93	0	0.63	0.045	0.19	0
5.85	0	1.21	0.086	0.37	0
11.7	0.39	2.25	0.16	0.67	0.30
29.3	0.96	4.62	0.33	1.35	0.98
58.5	1.21	7.07	0.50	2.01	1.64
176	1.55	10.6	0.76	2.91	2.54
293	1.57	11.8	0.84	3.19	2.82

$R_{rad}^{ion-pair}$ needs to be corrected by the value that corresponds to the starting point of the initiation process after oxygen inhibition (Table 4). This rate of initiation governs the rate of polymerization through the well-known equation:

$$R_p = \alpha\ (R_{rad}^{init})^{\beta} \quad (13)$$

where β corresponds to a term for the termination reactions (β = 1 for purely monomolecular reactions and β = 0.5 for purely bimolecular termination reactions) and α is a proportionality factor. For the formulation used, β was already found to be 0.65 for a comparable high-speed photoinitiating system. Consequently, the rate of polymerization R_p can be calculated and plotted against the power 0.65 of the rate of initiation $(R_{rad}^{init})^{0.65}$ (Fig. 2b). As can be seen, an excellent linear relationship is found, giving confidence to the conclusions drawn.

A decrease in the medium polarity should increase the association constant and, therefore, the concentration of ion-pairs. As a consequence, the rate of initiation should increase and the plateau region observed in Fig. 3b should be reached at a lower concentration of borate. Unfortunately, the limited solubility of IRT prevents this experiment.

3.4. Photobleaching study

A highly transparent polymer material is desired in many industrial applications. However, it is known that NIR dyes do not often lead to this desired property. However, bleaching experiments of photopolymers containing a PIS consisting of IRT and a borate salt as a coinitiator proved to be completely transparent in a range between 400 nm and 1000 nm, as shown in Fig. 6.

This experiment is in line with a previous report showing that after decomposition of the borate, the generated butyl radical can be added to the central double bond of the methine chain of the IRT molecule (Scheme 3).[24] The absorption spectrum of the expected photoproduct was computed at the TD-M062X/6-311++G**//B3LYP/6-31G* level. The maximum absorption band was found at 290 nm, thereby consolidating our conclusion. This reaction is similar to that already reported for cyanines/borate ion-pairs.[15]

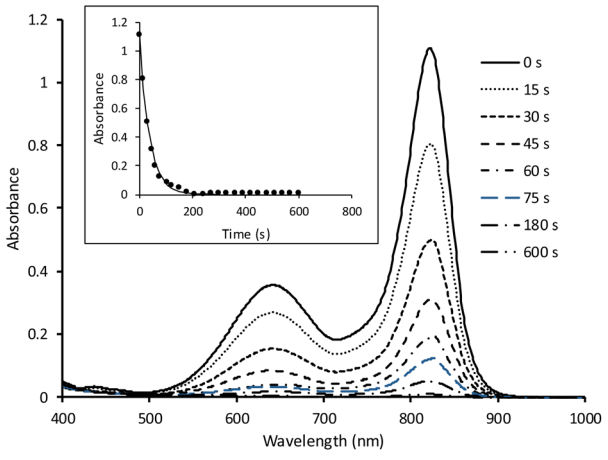

Fig. 6 Photolysis of IRT in 2-octanone in the presence of 1.76 × 10^{-2} M of borate B1 at different irradiation times (5 mW cm^{-2}). Inset: Corresponding photolysis decay observed at 823 nm and the best exponential decay fit.

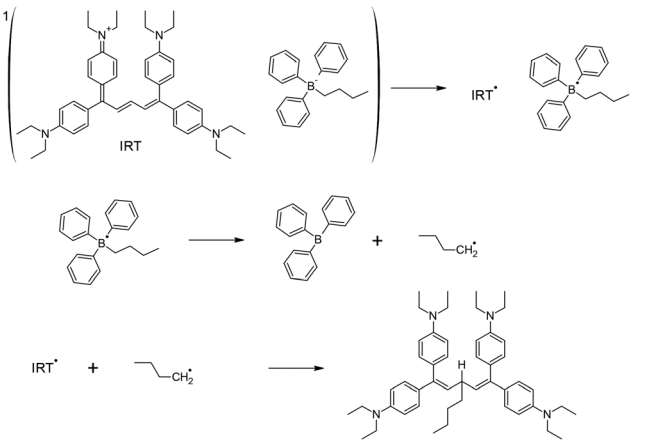

Scheme 3 Proposed mechanism for the photoreaction of IRT and borate salt B1 leading to complete photobleaching (adapted from ref. 21).

4. Conclusion

A radical photopolymerization in the NIR spectral region and at a low light intensity was performed using the polymethine dye IRT as a photoinitiator and borate salts as co-initiators. Furthermore, these photoinitiating systems were characterized in terms of their photochemical and physical properties. These studies revealed that IRT exhibits a very short singlet state lifetime, which prevents any efficient dynamical quenching known for conventional type II initiating systems. However, high rates of polymerization were still observed, suggesting that a different mechanism takes place. It was shown that this "atypical" mechanism is based on a pre-association between the dye cation and the borate anion. The equilibrium of this pre-association, as calculated from the Fuoss–Eigen equation, is strongly displaced in favor of the dye–borate complex. Light absorption by this complex leads immediately to the formation of initiating radicals. Only this static quenching can rationalize the high efficiency of the initiating system. As support for this hypothesis, the experimental rate of polymerization and the calculated rate of initiation at different concentrations of borates were found to be in good correlation. Finally, it was shown that the IRT/borate photoinitiating system leads to highly transparent photopolymerized films by virtue of a secondary process that decomposes the dye. The demonstrated characteristics make the IRT/borate photoinitiating system prone for usage in applications, where the initiation mechanism strictly has to be based on a photonic mechanism and where a high transparency of the photopolymer after photopolymerization is required, *e.g.* photopolymers for holographic applications.[33]

Conflicts of interest

There are no conflicts to declare.

References

1 A. Suerkan, E. A. Alkan, K. Kaya, Y. A. Udum, L. Toppare and Y. Yagci, *Prog. Org. Coat.*, 2021, **154**, 106189.
2 T. Brömme, C. Schmitz, N. Moszner, P. Burtscher, N. Strehmel and B. Strehmel, *ChemistrySelect*, 2016, **1**, 524–532.
3 B. Strehmel, C. Schmitz, T. Bromme, A. Halbhuber, D. Oprych and J. S. Gutmann, *J. Photopolym. Sci. Technol.*, 2016, **29**, 111–121.
4 Y. Pang, S. Fan, Q. Wang, D. Oprych, A. Feilen, K. Reiner, D. Keil, Y. L. Slominsky, S. Popov, Y. Zou and B. Strehmel, *Angew. Chem., Int. Ed.*, 2020, **59**, 11440.
5 C. M. Lin, S. M. Usama and K. Burgess, *Molecules*, 2018, **23**, 2900.
6 H. Liu, J. Yin, E. Xing, Y. Du, Y. Su, Y. Feng and S. Meng, *Dyes Pigm.*, 2021, **190**, 109327.
7 C. Kutahya, C. Schmitz, V. Strehmel, Y. Yagci and B. Strehmel, *Angew. Chem., Int. Ed.*, 2018, **57**, 7898–7902.
8 C. Schmitz, A. Halbhuber, D. Keil and B. Strehmel, *Prog. Org. Coat.*, 2016, **100**, 32–46.
9 C. Schmitz and B. Strehmel, *ChemPhotoChem*, 2017, **1**, 26–34.
10 Q. Wang, S. Popov, A. Feilen, V. Strehmel and B. Strehmel, *Angew. Chem., Int. Ed.*, 2021, **60**, 26855.
11 T. Brömme, C. Schmitz, D. Oprych, A. Wenda, V. Strehmel, M. Grabolle, U. Resch-Genger, S. Ernst, K. Reiner and D. Keil, *Chem. Eng. Technol.*, 2016, **39**, 13–25.
12 A. Caron, F. Dumur and J. Lalevée, *J. Polym. Sci.*, 2020, **58**, 2134–2139.
13 V. Launay, A. Caron, G. Noirbent, D. Gigmes, F. Dumur and J. Lalevée, *Adv. Funct. Mater.*, 2020, **31**, 2006324.
14 Y. Pang, A. Shiraishi, D. Keil, S. Popov, V. Strehmel, H. Jiao, J. S. Gutmann, Y. Zou and B. Strehmel, *Angew. Chem., Int. Ed.*, 2021, **60**, 1465–1473.
15 S. Chatterjee, P. Gottschalk, P. D. Davis and G. B. Schuster, *J. Am. Chem. Soc.*, 1988, **110**, 2326–2328.
16 M. C. Etter, B. N. Holmes, R. B. Kress and G. Filipoich, *Isr. J. Chem.*, 1985, **25**, 264–273.
17 B. Jędrzejewska, M. Pietrzak and Z. Rafiński, *Polymer*, 2011, **52**, 2110–2119.
18 A. Ibrahim, X. Allonas, C. Ley, K. Kawamura, H. Berneth, F. K. Bruder, T. Fäcke, R. Hagen, D. Hönel and T. Rölle, *Chem. – Eur. J.*, 2014, **20**, 15102–15107.
19 T. Roelle, H. Berneth, D. Hoenel and F. K. Bruder, Process for the production of triaryl organoborate salts with organic cations as photoinitiators of radical polymerization, WO2018087062A1, 2018.
20 T. Roelle, H. Berneth, D. Hoenel, F. K. Bruder and J. Kintrup, Method for producing triarylorganoborates, WO2018087064A1, 2018.
21 T. Roelle, G. Satyanarayana, S. Roychowdhury, R. M. Patil and A. K. A. Pillar, Process for the manufacturing of triarylorgano borates, WO2018099698A1, 2018.
22 J. Christmann, X. Allonas, C. Ley and C. Croutxé-Barghorn, *Polym. Chem.*, 2019, **10**, 1099–1109.
23 P. Jacques, D. Burget and X. Allonas, *New J. Chem.*, 1996, **30**, 933.
24 M. Matsuoka and T. Hikida, *Mol. Cryst. Liq. Cryst. Sci. Technol., Sect. A*, 1993, **227**, 309–315.
25 K. Murofushi and Y. Hosoda, EP438123A2, 1991.
26 S. Strickler and R. A. Berg, *J. Chem. Phys.*, 1962, **37**, 814–822.
27 R. C. Hilborn, *Am. J. Physiol.*, 1982, **50**, 982–986.
28 W. R. Ware and B. A. Baldwin, *J. Chem. Phys.*, 1964, **40**, 1703–1705.
29 C. Ley, P. Bordat, L. Di Stefano, L. Remongin, A. Ibrahim, P. Jacques and X. Allonas, *Phys. Chem. Chem. Phys.*, 2015, **17**, 5982–5990.
30 M. Eigen, *Z. Phys. Chem.*, 1954, **1**, 176–200.
31 R. M. Fuoss, *J. Am. Chem. Soc.*, 1958, **80**, 5059–5061.
32 P. Hemmes, *J. Am. Chem. Soc.*, 1972, **94**, 75–76.
33 Exemplary information on Bayfol® HX product line is given in Friedrich-Karl Bruder, Johannes Frank, Sven Hansen, Alexander Lorenz, Christel Manecke, Richard Meisenheimer, Jack Mills, Lena Pitzer, Igor Pochorovski, Thomas Rölle, "Expanding the property profile of Bayfol HX(R) film towards NIR recording and ultra-high index modulation", Proc. SPIE 11710, Practical Holography XXXV: Displays, Materials, and Applications, 1171003 (5 March 2021).